Epibranchial ganglia orchestrate the development of the cranial neurogenic crest

Eva Coppola[a], Murielle Rallu[a,1], Juliette Richard[a,2], Sylvie Dufour[b], Dieter Riethmacher[c], François Guillemot[d], Christo Goridis[a], and Jean-François Brunet[a,3]

[a]Institut de Biologie de l'Ecole Normale Supérieure (IBENS), Centre National de la Recherche Scientifique UMR8197, Institut National de la Santé et de la Recherche Médicale U1024, 75005 Paris, France; [b]Institut Curie, Centre National de la Recherche Scientifique Unité Mixte de Recherche 144, 75005 Paris, France; [c]University of Southampton, School of Medicine, Southampton SO16 6YD, United Kingdom; and [d]National Institute for Medical Research, London NW71AA, United Kingdom

Edited by Joshua R. Sanes, Harvard University, Cambridge, MA, and approved December 22, 2009 (received for review September 10, 2009)

The wiring of the nervous system arises from extensive directional migration of neuronal cell bodies and growth of processes that, somehow, end up forming functional circuits. Thus far, this feat of biological engineering appears to rely on sequences of pathfinding decisions upon local cues, each with little relationship to the anatomical and physiological outcome. Here, we uncover a straightforward cellular mechanism for circuit building whereby a neuronal type directs the development of its future partners. We show that visceral afferents of the head (that innervate taste buds) provide a scaffold for the establishment of visceral efferents (that innervate salivatory glands and blood vessels). In embryological terms, sensory neurons derived from an epibranchial placode—that we show to develop largely independently from the neural crest—guide the directional outgrowth of hindbrain visceral motoneurons and control the formation of neural crest–derived parasympathetic ganglia.

autonomic nervous system | epibranchial placode | neural circuit | *Phox2b* | neural crest

During ontogeny of the nervous system, neuronal cell bodies and processes undergo extensive directional migrations or growths. From both a developmental and evolutionary perspective, it would seem to make sense that the migrating somata and processes of neurons destined to a given circuit would be guided, at least in part, by other partners of the same circuit. However, documented examples of this intuitive way of wiring the brain are few and far between and most identified guidance cues emanate from structures that do not participate in the final connectivity of the system (1, 2). The few exceptions, thus far, include homotypic interactions between pioneers and followers or between peers in axonal tracts (3), the towing of the lateral line-nerve growth cones by their future targets in zebrafish (4), and the guidance of sensory fibers by motor ones in spinal nerves (5). An attractive model to look for such navigational cues among future partners of the same circuit is offered by the visceral neurons of the vertebrate head, which display a high degree of anatomic promiscuity, whereby mixed sensory and motor nerves are formed and motor or sensory nerves traverse sensory or motor ganglia, respectively: this tangled anatomy suggests that some neurons might depend on others for their development or guidance. In this study, we focused on the facial nerve (nVII) (see schematic; Fig. 1). The sensory fibers of nVII emanate from the viscerosensory neurons of the geniculate ganglion. These neurons, primarily concerned with taste, project centrally to the nucleus of the solitary tract (nTS) and peripherally to taste buds through the greater superficial petrosal nerve (GSPN) and the corda tympani (CT). The motor fibers of nVII are of two types: visceromotor and branchiomotor. The visceromotor axons emanate from the salivatory motoneurons of the hindbrain, traverse the geniculate ganglion, and course in the GSPN and CT to synapse on parasympathetic neurons of the sphenopalatine ganglion (Spg) and the submandibular and lingual ganglia (S/Lg), respectively, which innervate, among others, salivatory glands and blood vessels of the oral cavity. The mixed sensorimotor GSPN is joined by sympathetic fibers from the superior cervical ganglion. Finally, the branchiomotor fibers emanate from the facial motor nucleus, traverse the geniculate ganglion and, after the emergence of the CT, form the main branch of the facial nerve that innervates facial muscles. From a developmental standpoint, this circuitry involves all three canonical sources of neural tissue in vertebrates: the visceromotor neurons are born in the neural tube; the viscerosensory neurons are derived from an epibranchial placode; parasympathetic and sympathetic ganglia arise from the neural crest. Despite their varied origins and phenotypes, all these structures express the homeodomain transcription factors *Phox2a* and *Phox2b*, on which they depend for their differentiation (6). We thus engineered conditional null alleles of *Phox2a* and *Phox2b* (Fig. S1) to selectively alter or ablate individual neuron-types of the head visceral circuits and monitor the consequence on others.

Results

Neither Visceromotor nor Viscerosensory Neurons Require Parasympathetic Ganglia. We first tested the possibility that the parasympathetic precursors of the Spg or S/Lg could guide the axonal growth of their presynaptic partner, the visceromotor neurons. We examined *Phox2a* knockouts, in which the Spg is missing (7), as well as the S/Lg, albeit with a weaker penetrance (Fig. 1 *A* and *B*). We confirmed the finding (8) that these mutants also lack the GSPN, which normally projects to the Spg, and in addition found that some embryos lacked the CT, which normally projects to the S/Lg (Fig. 1 *A′* and *B′*). This could suggest that the lack of GSPN and CT, including their motor fibers, ensues from the absence of the latter's target, the Spg and S/Lg (8). This interpretation, however, cannot be supported by simple *Phox2a* knockouts, in which *Phox2a* is inactivated in all three cell-types: visceromotor, viscerosensory, and ganglionic parasympathetic. We thus used a spatially controlled knockout strategy (Fig. S1). First, we inactivated *Phox2a* selectively in neural crest derivatives (Fig. S1) (including parasympathetic precursors) with a *Cre* transgene driven by the *Wnt1* promoter (9). Unexpectedly, in *Wnt1::Cre;Phox2a*$^{lox/lox}$ embryos, all head parasympathetic ganglia formed (Fig. 1*C*). This showed that their disappearance in *Phox2a* knockouts (7) (Fig. 1*B*) is a noncell-autonomous effect. As expected, both GSPN and CT were also

Author contributions: E.C., C.G., and J.-F.B. designed research; E.C., M.R., and J.R. performed research; S.D., D.R., and F.G. contributed new reagents/analytic tools; E.C., C.G., and J.-F.B. analyzed data; and E.C. and J.-F.B. wrote the paper.

The authors declare no conflict of interest.

This article is a PNAS Direct Submission.

[1]Present address: Sanofi-Aventis R&D, 94403 Vitry sur Seine, Cedex, France.

[2]Present address: Eli Lilly France, 95150 Suresnes, France

[3]To whom correspondence should be addressed. E-mail: jfbrunet@biologie.ens.fr.

This article contains supporting information online at www.pnas.org/cgi/content/full/0910213107/DCSupplemental.

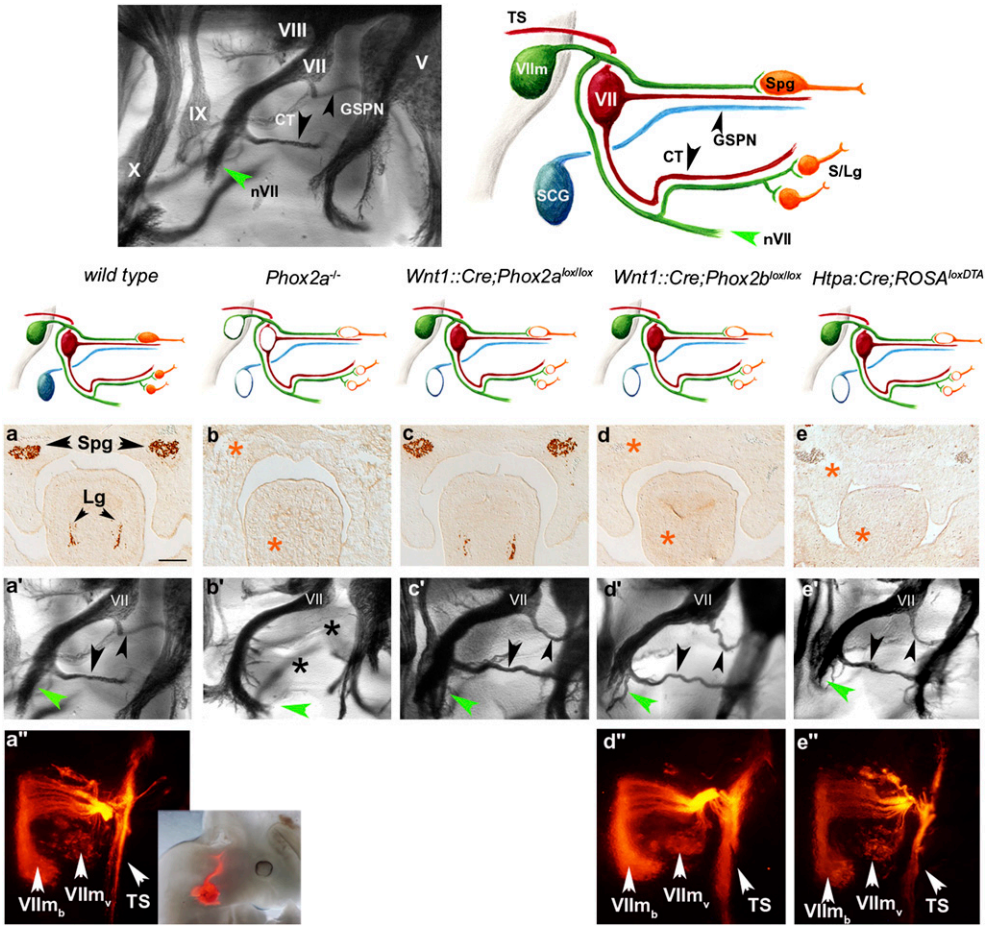

Fig. 1. Viscerosensory and visceromotor neurons project in the absence of parasympathetic ganglia. (*Upper Left*) Neurofilament stain of the facial nerve complex at E11.5 and (*Right*) schematic at E13.5. (*Lower*) Phenotype of the head parasympathetic ganglia and branches of the geniculate ganglion in the indicated genetic backgrounds (*Rosa*^{locDTA} stands for *Rosa*$^{lox\text{-}stop\text{-}lox\text{-}DTA}$). The schematics depict the structures in whose precursors the gene has been inactivated or where DTA was expressed as hollowed-out shapes (and do not represent the phenotype). (*A*–*E*) Transverse sections through the head of E13.5 (*A*–*D*) or E12.5 (*E*) embryos stained by immunohistochemistry for Phox2b (*A*–*C* and *E*) or Phox2a (d) to detect the Spg and lingual ganglia (the submandibular proper is in another plane of section). An orange asterisk indicates their absence. (*A′*–*E′*), Neurofilament stain of the facial nerve and its branches at E11.5. The GSPN and CT are indicated by an upward or downward black arrowhead, respectively, and their absence by a black asterisk. The main branch of the facial nerve is indicated by a green arrowhead. (*A″*, *D″*, *E″*), Flat-mounted E11.5 hindbrain retrogradelly labeled with DiI placed in the second branchial arch (*Inset*). V, VII, VIII, IX, and X: trigeminal, geniculate, statoacoustic, petrosal, and nodose ganglia. $VIIm_b$, branchial motoneurons of the facial nucleus; $VIIm_v$, visceral motoneurons of the salivatory nucleus; CT, corda tympani; GSPN, greater superficial petrosal nerve; nVII, facial nerve; SCG, superior cervical ganglion, S/Lg, submandibular and lingual ganglia; Spg, sphenopalatine ganglion; TS, tractus solitarius. (Scale bar, 200 μm.)

present (Fig.1*C′*). In contrast, inactivation of *Phox2b* by the *Wnt1::Cre* allele resulted in the disappearance of all head parasympathetic ganglia (Fig. 1*D*), verifying that their dependence on *Phox2b* (10) is cell-autonomous. Unexpectedly however, in *Wnt1::Cre;Phox2b*$^{lox/lox}$ embryos, both the GSPN and CT (that normally project toward the Spg and S/Lg) appeared normal at E11.5 (Fig. 1*D′*). Moreover, the facial nerve had retained its mixed viscerosensory and visceromotor nature, as demonstrated by retrograde labeling with DiI, which revealed the cell bodies of facial and salivatory motoneurons and the solitary tract (Fig. 1*A″* and *D″*).

We then asked whether parasympathetic precursors in which *Phox2b* is inactivated could still play a role in GSPN and CT formation before their demise, by visualizing them with X-gal staining in a *Wnt1::Cre;Phox2b*$^{LacZ/lox}$ background. At E12.5, a few scattered $LacZ^+$ parasympathetic precursors were detectable at the position of the future Spg (Fig. S6). Thus, even though *Phox2b*-depleted parasympathetic precursors never form a Spg, at least a few migrate to their final location and could steer branches of the facial nerve. To rule out this possibility, we ablated the parasympathetic precursors at an earlier stage, before they have switched on *Phox2b* expression. In a first experiment, we partnered a *Cre* transgene under the control of the *Htpa* promoter [which is expressed in neural crest cells right after their epithelial-mesenchymal transition (11)], with an allele conditionally expressing diphteria toxin subunit A (DTA) from the *Rosa* locus (12). As expected, in *Htpa::Cre;Rosa*$^{lox\text{-}stop\text{-}lox\text{-}DTA}$ mutants, no parasympathetic precursor was detectable at E12.5 (Fig. 1*E*). However, at E11.5 the geniculate ganglion appeared normal, as well as the GSPN, CT, and the main branch of the facial nerve (Fig. 1*E′*). Retrograde filling with DiI verified that both viscerosensory and visceromotor fibers were present (Fig. 1*E″*). Finally, we triggered DTA expression in the neural crest at an even earlier stage—before migration (13)—in a *Wnt1::Cre;Rosa*$^{lox\text{-}stop\text{-}lox\text{-}DTA}$ background. Although numerous anomalies were evident in the branching pattern of the facial nerve, attributable at least in part to the grossly disorganized environment in which they grow (Fig. S3), a CT and a GSPN could be spotted (Fig. 2 *A* and *B*). Altogether, these results show that neither viscerosensory nor visceromotor neurons require the parasympathetic ganglia to grow their normal peripheral projections.

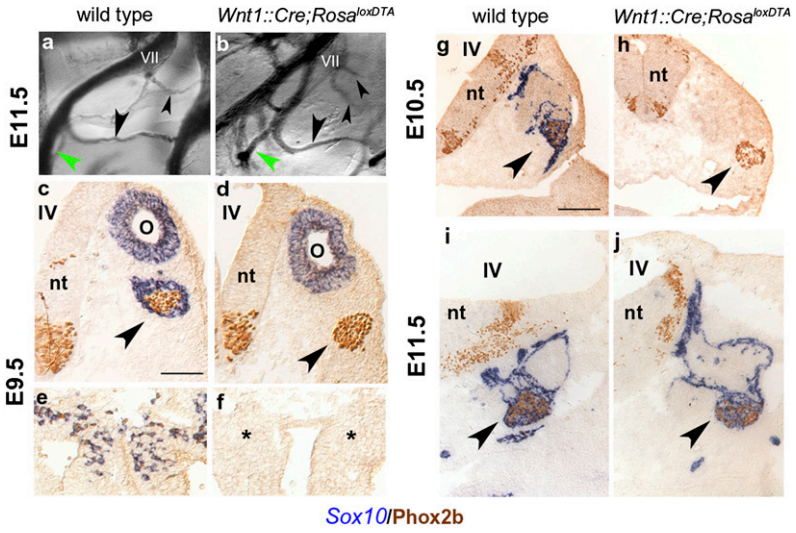

Fig. 2. Early ablation of neural crest does not affect the formation of the geniculate ganglion and reveals an alternate source of glial cells. (*A* and *B*) Whole-mount neurofilament staining of the facial nerve branches in wild-type and *Wnt1::Cre; Rosa*$^{lox\text{-}stop\text{-}lox\text{-}DTA}$ embryos. The GSPN and CT are indicated by black arrowheads, respectively upward and downward. In that particular mutant the GSPN appears duplicated. The main branch of the facial nerve is indicated by a green arrowhead. (*C–J*)Transverse sections of wild type and *Wnt1::Cre; Rosa*$^{lox\text{-}stop\text{-}lox\text{-}DTA}$ embryos at the indicated stages, at the level of the geniculate ganglion (*C*, *D*, and *G–J*) or trunk (*E* and *F*), hybridized with a *Sox10* probe (*blue*), followed by Phox2b immunohistochemistry (*orange*). The black arrowheads indicate the geniculate ganglion. The black asterisks in *F* show the absence, in *Wnt1::Cre; Rosa*$^{lox\text{-}stop\text{-}lox\text{-}DTA}$ embryos, of Phox2b^{+}/*Sox10*$^{+}$ enteric neurons. nt, neural tube; O, otic vesicle; IV, fourth ventricle; VII, geniculate ganglion. [Scale bar: (*C–F*), 100 μm; (*G–I*): 200 μm.]

Epibranchial Ganglia Form in the Absence of Neural Crest. The previous experiments, in which presumably all neural crest cells are ablated along with parasympathetic precursors, led us to revisit the larger issue of the role of neural crest in the formation of epibranchial ganglia. Although it is well established that the neural crest contributes glia to the epibranchial ganglia (14), it was described in chicken that the geniculate ganglion forms, as well as all its peripheral branches, after extirpation of the neural crest (15, 16). Later on, however, similar surgical experiments were reported to impede the inward migration, aggregation, and central axonal outgrowth of geniculate placodal neuronal precursors (17). As described above, in crosses of *Htpa::Cre* or *Wnt1::Cre* alleles with a *Rosa*$^{lox\text{-}stop\text{-}lox\text{-}DTA}$ allele, the epibranchial ganglia retained to a degree their capacity to grow peripheral projections (Figs. 1*E′* and 2*B*). We therefore monitored ganglion formation at earlier stages in these mutant backgrounds while verifying the efficacy of neural crest depletion by in situ hybridization for *Sox10*. In wild-type embryos at E9.5, *Sox10* cells were visible in cranial ganglia (Fig. 2*C*), as well as in enteric ganglia (Fig. 2*E*). In *Htpa::Cre;Rosa*$^{lox\text{-}stop\text{-}lox\text{-}DTA}$ at the same stage, *Sox10*$^{+}$ cells were also present in these structures (Fig. S2). Thus, the killing of crest cells by DTA in *Htpa::Cre;Rosa*$^{lox\text{-}stop\text{-}lox\text{-}DTA}$ embryos occurred late enough for some neuroglial precursors to reach the epibranchial ganglia, and conceivably fulfill their proposed role (17) in the delamination and aggregation of placodal cells. In contrast, in *Wnt1::Cre;Rosa*$^{lox\text{-}stop\text{-}lox\text{-}DTA}$ embryos, *Sox10*$^{+}$ cells were detectable neither in epibranchial ganglia (Fig.2*D*) nor in the trunk of the embryo (Fig. 2*F*) at E9.5. Despite the absence of *Sox10*$^{+}$ cells, geniculate ganglia had formed at their normal location (Fig. 2*D*).

Surprisingly, *Sox10*$^{+}$ cells, still undetectable at E10.5 (Fig. 2 *G* and *H*), had appeared at E11.5 in the geniculate ganglia of *Wnt1::Cre; Rosa*$^{lox\text{-}stop\text{-}lox\text{-}DTA}$ embryos (Fig. 2 *I* and *J*), while the efficacy of neural crest ablation was attested, at the same stage, by the absence of *Sox10*$^{+}$ cells in any other locations where they are normally found: the dorsal root ganglia, the sympathetic chain, and even the enteric nervous system, which is derived from the same axial level than the glia destined to epibranchial ganglia (Fig. S3). However, we cannot exclude that these late appearing *Sox10*$^{+}$ cells represent an atypical contingent of cranial crest cells somehow spared by the *Wnt1::Cre;Rosa*$^{lox\text{-}stop\text{-}lox\text{-}DTA}$ allele (e.g., which would not express *Wnt1*, or only transiently or belatedly); alternatively, they might come from the neural tube, known to give off glia to motor roots in the spinal cord (18); finally, the placodes themselves might serve as a compensatory source of *Sox10* cells in the absence of neural crest. Whatever the case, these findings indicate that in mouse, the epibranchial ganglia can form and grow peripheral projections in the absence of early (E9–E10) neural crest-derived *Sox10*$^{+}$ immigrants.

Neither Parasympathetic Ganglionic nor Viscerosensory Neurons Require Visceromotor Neurons. Having shown that visceromotor fibers do not need their target (i.e., the parasympathetic ganglia) to navigate, we asked whether, conversely, the parasympathetic ganglia require their presynaptic partner (i.e., the visceromotor neurons) to form. We selectively inactivated *Phox2b* in visceromotor neurons with a *Brn4::Cre* allele, which is expressed throughout the CNS (19). In *Brn4::Cre;Phox2b*$^{lox/lox}$ embryos, visceromotor neurons were not born (Fig. S4), confirming that they require *Phox2b* cell-autonomously (20). Nonetheless, in the periphery, the Spg and S/Lg had formed at E13.5 (Fig. 3*A*), showing that the parasympathetic ganglia do not require the visceromotor neurons to form. In addition, the GSPN and CT were present (Fig. 3*A′*) although formed exclusively of sensory fibers, as shown by DiI retrograde labeling (Fig. 3*A″*). This shows that the viscerosensory neurons do not need the visceromotor neurons for directional axonal outgrowth. Surprisingly, in Brn4::Cre;Phox2b$^{lox/lox}$ embryos, just as in simple *Phox2b* knockouts, the main trunk of the facial nerve (classically considered as purely motor) was present, despite the absence of visceral or branchial motoneurons (Fig. 3 *A′* and *C′*). This residual contingent of fibers might include the somatic sensory component of the facial nerve (forming the posterior auricular nerve and destined to the external ear), the small (8%) proportion of all facial sensory fibers found to course in the main "motor" trunk of the nerve in cat (21), or previously undescribed sensory projections, permanent or transient—and of unknown origin—in the facial nerve trunk of mice.

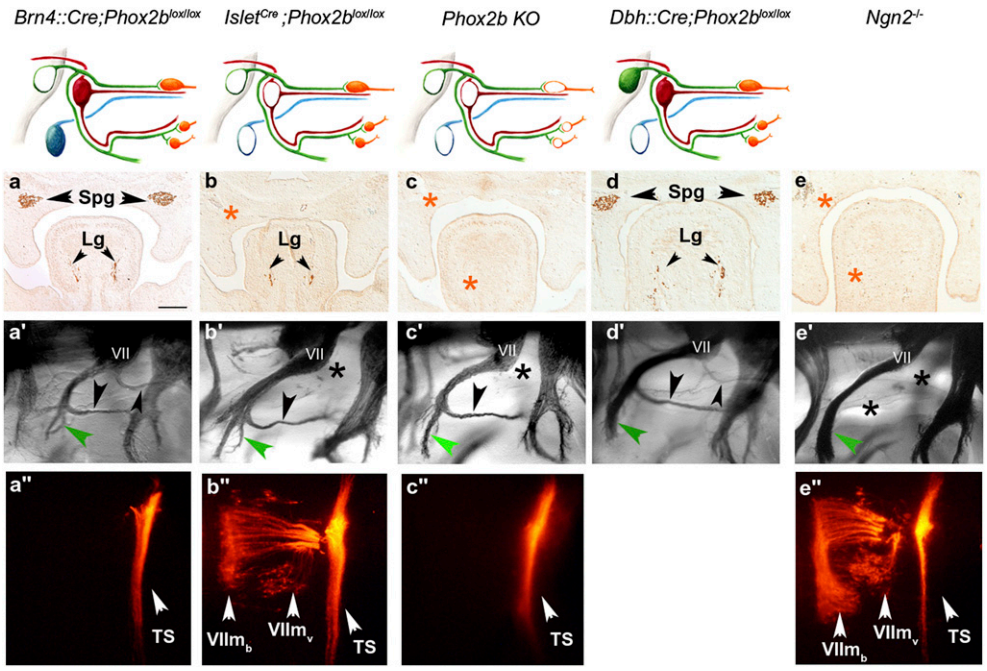

Fig. 3. The geniculate ganglion organizes the parasympathetic innervation of the head. For each genotype, the schematic indicates which structures *Phox2b* has been deleted from as hollowed out shapes (and do not represent the phenotype). (*A*–*E*) Transverse sections through the head of E13.5 embryos stained by immunohistochemistry for Phox2b (*A*, *B*, *D*, *and E*) or Phox2a (*C*) to detect the Spg and lingual (Lg) ganglia. Their absence is indicated by an orange asterisk. (*A′*–*E′*) Lateral view of the geniculate ganglion and its branches on whole-mount neurofilament stains of E11.5 embryos. The GSPN and CT are indicated by an upward and downward black arrowhead, respectively, and their absence by a black asterisk. A green arrowhead points to the main branch of the facial nerve. (*A″*, *B″*, *C″*, and *E″*) Retrograde DiI labeling of motor neurons and sensory projections from the second branchial arch in the indicated genetic background. VII, geniculate ganglion; VIIm$_b$, branchial motoneurons of the facial nucleus; VIIm$_v$, visceral motoneurons of the salivatory nucleus; CT, corda tympani; GSPN, greater superficial petrosal nerve; Lg, lingual ganglia, Spg: sphenopalatine ganglion; TS, tractus solitarius. (Scale bar, 200 μm.)

Both Visceromotor and Parasympathetic Ganglionic Neurons Require Viscerosensory Neurons. We finally asked whether the parasympathetic neural crest depends on the viscerosensory neurons. Because *Ngn2* is expressed in epibranchial placodes (22), we first considered the use of an *Ngn2::Cre* allele to delete *Phox2a* or *Phox2b* from geniculate sensory precursors which express both genes (23), and partially depend on them (7, 10, 24). However, both a transgenic *Ngn2::CreERT2* line (25) and an *Ngn2^{CreERT2}* knock-in line (kind gift of Giacomo Consalez, DIBIT, Milan, Italy), showed weak expression in the peripheral nervous system and scarcely any in the epibranchial ganglion precursors when crossed with a reporter, which precluded the use of this strategy. We thus turned to a *Cre* recombinase expressed from the *Islet1* locus (26) which, based on the *Islet1* expression pattern, should delete *Phox2b* in epibranchial placodes (27), in postmitotic visceromotor neurons (28), and in sympathetic ganglia (29), but not in parasympathetic ganglia. Indeed, neither endogenous *Islet1* expression nor reporter gene expression in a *Islet^{Cre};Tau$^{lox\text{-}stop\text{-}loxNlsLacZ}$* background was detected in parasympathetic ganglia at E13.5 (Fig. S5). Despite the lack of *Islet^{Cre}* expression in parasympathetic precursors, the Spg failed to form in *Islet^{Cre};Phox2b$^{lox/lox}$* embryos (on six sides out of eight, in four embryos), but the S/Lg were present (Fig. 3*B*). In parallel, the GSPN was missing (on five sides out of six, in three embryos), but not the CT (Fig. 3*B′*), just like in the *Phox2b* knockouts (Fig. 3*C′*). This shows that, at early stages, *Phox2b* is selectively required in the geniculate ganglion for the formation of the GSPN, and also, both cell-autonomously (Fig. 1*D*) and non-cell-autonomously for that of the Spg. The site of *Phox2b* non-cell-autonomous action on the Spg could be either the geniculate ganglion, or the visceromotor neurons, or the superior cervical ganglion that all express *Islet^{Cre}*, and all project to or through the Spg (Fig.1). Our previous observation that *Brn4::Cre;Phox2b$^{lox/lox}$* embryos, devoid of motoneurons, have a normal Spg (Fig. 3*A*), and the fact that *Islet^{Cre};Phox2b$^{lox/lox}$* (who lack a Spg) have a normal contingent of visceral motoneurons (Fig. 3*B″*, compare with Fig.1*A″*), excludes the latter as the culprit. We thus inactivated *Phox2b* selectively in the superior cervical ganglion with a *Dbh::Cre* allele (30). Again, both GSPN and Spg developed normally (Fig. 3 *D* and *D′*). By exclusion, we conclude that the formation of both GSPN and Spg require *Phox2b* expression in the geniculate ganglion.

To confirm by other means that the integrity of the geniculate ganglion is required for the formation of parasympathetic ganglia, we examined *Ngn2* knockout mice. *Ngn2* is expressed in epibranchial placodes and required for the formation of the geniculate ganglion (22). In E13.5 *Ngn2* knockout embryos, all parasympathetic ganglia of the head were missing (Fig. 3*E*). In addition, neither the CT nor the GSPN had formed at E11.5 (Fig. 3*E′*). We verified that *Ngn2* is not expressed in parasympathetic ganglia (Fig. S5), nor is it expressed in visceromotor or sympathetic neurons (31, 32), although we cannot exclude that it is transiently expressed in Spg precursors. Notwithstanding this limitation, the *Ngn2* knockout provides further evidence that genetic damage to the geniculate ganglion blocks the formation of head parasympathetic ganglia. Surprisingly, retrograde filling revealed a solitary tract (Fig. 3*E″*), showing that sensory fibers project in the main branch of the facial nerve of *Ngn2* knockout embryos. The source of these fibers is unknown and might reflect the delayed formation of a geniculate ganglion previously described at E12.5 in *Ngn2* knockouts (22), which, however, rescues neither the GSPN nor the CT. A normal contingent of visceromotor neurons was also evident (Fig. 3*E″*), indicating that in the absence of both GSPN and CT the visceromotor neurons project abnormally in the main branch of the facial nerve, and thus require the viscerosensory fibers to navigate properly.

Discussion

Our data show that an intact geniculate ganglion is required for the formation of head parasympathetic ganglia and the establishment of their preganglionic innervation. In neuroanatomical terms, this amounts to an intriguing case of self-assembly of a reflex circuit, whereby its afferent pathway (specialized in taste reception) instructs the development of its efferent pathway (that vasodilates blood vessels of the mouth and stimulates salivatory glands).

By far the simplest underlying mechanism would be that the axons of the viscerosensory neurons serve as a migration route for both the crest-derived parasympathetic precursors and visceromotor axons. In support of this hypothesis, there was a good correlation between the disappearance of individual branches of the facial nerve (GSPN and CT) and that of their associated ganglia: in $Islet^{Cre}$;$Phox2b^{lox/lox}$ embryos only the GSPN is missing and, correlatively, only the Spg fails to form. In *Phox2a* knockout embryos the loss of the Spg and GSPN was fully penetrant, that of the CT and S/Lg inconstant. In *Ngn2* knockout embryos, both GSPN and CT were missing, together with all parasympathetic ganglia. Also suggestive of a guiding role for projections of the geniculate ganglion are previous observations that lingual ganglionic precursors first appear in the tongue surrounding fibers from the geniculate (33). Further evidence comes from the transient detection of parasympathetic precursors at the site of Spg formation in *Wnt1::Cre*;$Phox2b^{LacZ/lox}$ embryos (in which the GSPN forms) but not in simple *Phox2b* knockouts (in which GSPN formation is prevented) (Fig. S6). This shows that before the formation of the Spg proper, the migration of parasympathetic precursors to the site of ganglion formation depends on an intact GSPN. It is tempting to hypothesize that this guiding mechanism holds true for trunk parasympathetic ganglia, which form in close association with branches of the vagus nerve (34, 35).

The dependency of the efferent visceral pathway (visceromotor fibers and their neural crest-derived ganglionic targets) on the afferent pathway (the viscerosensory neurons), suggests that the latter predates the former in evolution. In line with this, there is no report of parasympathetic ganglia associated with the facial nerve in cyclostomes, elasmobranches, or teleost fish (except, in selachian elasmobranches, for its hyomandibular — but neither palatine nor mandibular—branch) (36), and indeed, no salivatory gland in fish. It could be that the original efferent pathway coupled with taste reception was represented by the sole branchiomotor neurons whose existence precedes vertebrates (37) and that motorize the jaw and pharyngeal muscles. The visceromotor pathways would have then arisen in land vertebrates, using the scaffold of the gustatory pathways.

Materials and Methods

Mouse Strains. To generate the conditional *Phox2a* ($Phox2a^{Lox}$) and *Phox2b* ($Phox2b^{Lox}$) mice, we engineered two targeting constructs containing the *Phox2a* or *Phox2b* exon 2 flanked by *loxP* sites and including a nearby neoresistance marker (see Fig. S1 for the detailed strategy). The targeting constructs were electroporated into CK35 embryonic stem cells of *129SvPas* origin. Correctly targeted embryonic stem cells were expanded, confirmed by Southern blotting (Fig. S1), and injected into blastocysts (Service d'Expérimentation Animale et de Transgénèse) to generate chimeras that transmitted the mutant allele through the germ line. The agouti offspring of the chimeras were genotyped by PCR using the following primers: for $Phox2a^{Lox}$: GCCTCCAACTCCATATTCC and ATCAGGAGTCAGTCGTCTG; for $Phox2b^{Lox}$: GGCCGGTCATTTTTATGATC and AAGTGCCTTTGGGTGAGATG. The primers flanked either the 3′ (for *Phox2a*) or 5′ (for *Phox2b*) *loxP* site. The neomycin resistance cassette was removed by crossing with a *Flpe* deleter allele (38). The resulting heterozygous $Phox2b^{lox/+}$ or $Phox2a^{lox/+}$ mice were intercrossed to produce homozygous $Phox2a^{lox/lox}$ or $Phox2b^{lox/lox}$ mice, which were viable and fertile and without obvious phenotype. To obtain all of the experimental models used in this study, the following transgenic lines were used: *Wnt1::Cre* (9), $Islet^{Cre}$ (26), *Brn4::Cre* (19), *Dbh::Cre* (30), *HtpA::Cre* (11); *Phox2a* (8), *Phox2b* (10) and *Ngn2* (22) knockouts; the reporter line $Tau^{lox\text{-}stop\text{-}loxNlsLacZ}$ (39), and the $Rosa^{lox\text{-}Stop\text{-}lox\text{-}DTA}$ (12) line. All animal studies were done in accordance with the guidelines issued by the French Ministry of Agriculture and have been approved by the Direction départementale des services vétérinaries de Paris.

Histology. The methods for in situ hybridization and immunostaining have been described (40). All of the probes [*Sox10* (gift of M. Wegner, Emil-Fischer-Zentrum, Germany), *Peripherin*, and *Ngn2* (gift of F. Guillemot, NIMR, UK)] were synthesized using a DIG RNA labeling kit (Roche) as specified by the manufacturer. The primary antibodies used were: rabbit anti-Phox2a (40), rabbit anti-Phox2b (23), mouse anti-Islet1/2 (40.2D6 and 39.4D5, Developmental Study Hybridoma Bank), mouse anti-Neurofilament (2H3, Developmental Study Hybridoma Bank). The primary antibodies were revealed for bright field observation by biotin-labeled secondary antibodies using a Vectastain ABC kit.

For X-Gal staining, the embryos were treated as described in ref. 41. Whole-mount immunohistochemistry was done as in ref. 42, using the anti-neurofilament 2H3 antibody and a peroxidase-conjugated anti-mouse antibody (Sigma).

DiI tracing was carried out by placing a single crystal of fluorescent carbocyanide dye in the second branchial arch of E11.5 embryos previously fixed in 4% buffered paraformaldehyde. The dye was let to diffuse for 1 week at room temperature in 4% paraformaldehyde, then the embryos were dissected, and the hindbrains photographed under fluorescent light.

For detection of parasympathetic ganglia on sections and of branches of the facial nerve by whole-mount immunohistochemistry, at least the two sides of two animals of each genotype were examined. The phenotype was fully penetrant in all cases, except when mentioned otherwise.

ACKNOWLEDGMENTS. We thank G. Schütz (DKFZ, Heidelberg) for the *Dbh::Cre* line, C. Birchmeier (MDC, Berlin) and E. B. Crenshaw (Children's Hospital of Philadelphia, Philadelphia) for the *Brn4::Cre* line, and Sylvia Arber (Biozentrum, Basel) fo the $Tau^{lox\text{-}stop\text{-}loxNlsLacZ}$ and the $Islet^{Cre}$ lines. This work was supported by grants from the Agence Nationale de la Recherche and the Fondation pour la Recherche Médicale (to J.-F.B.) and institutional support from the Centre National de la Recherche Scientifique.

1. Song H, Poo M (2001) The cell biology of neuronal navigation. *Nat Cell Biol* 3:E81–E88.
2. Chao DL, Ma L, Shen K (2009) Transient cell-cell interactions in neural circuit formation. *Nat Rev Neurosci* 10:262–271.
3. Pittman AJ, Law MY, Chien CB (2008) Pathfinding in a large vertebrate axon tract: isotypic interactions guide retinotectal axons at multiple choice points. *Development* 135:2865–2871.
4. Gilmour D, Knaut H, Maischein HM, Nüsslein-Volhard C (2004) Towing of sensory axons by their migrating target cells in vivo. *Nat Neurosci* 7:491–492.
5. Landmesser L, Honig MG (1986) Altered sensory projections in the chick hind limb following the early removal of motoneurons. *Dev Biol* 118:511–531.
6. Brunet J-F, Goridis C (2008) Phox2b and the homeostatic brain. *Genetic Basis for Respiratory Control Disorders*, ed Gaultier C (Springer, New York), pp 25–44.
7. Morin X, et al. (1997) Defects in sensory and autonomic ganglia and absence of locus coeruleus in mice deficient for the homeobox gene *Phox2a*. *Neuron* 18:411–423.
8. Jacob J, Tiveron M-C, Brunet J-F, Guthrie S (2000) Role of the target in the pathfinding of facial visceral motor axons. *Mol Cell Neurosci* 16:14–26.
9. Danielian PS, Muccino D, Rowitch DH, Michael SK, McMahon AP (1998) Modification of gene activity in mouse embryos in utero by a tamoxifen-inducible form of Cre recombinase. *Curr Biol* 8:1323–1326.
10. Pattyn A, Morin X, Cremer H, Goridis C, Brunet J-F (1999) The homeobox gene *Phox2b* is essential for the development of autonomic neural crest derivatives. *Nature* 399:366–370.
11. Pietri T, Eder O, Blanche M, Thiery JP, Dufour S (2003) The human tissue plasminogen activator-Cre mouse: a new tool for targeting specifically neural crest cells and their derivatives in vivo. *Dev Biol* 259:176–187.
12. Brockschnieder D, Pechmann Y, Sonnenberg-Riethmacher E, Riethmacher D (2006) An improved mouse line for Cre-induced cell ablation due to diphtheria toxin A, expressed from the Rosa26 locus. *Genesis* 44:322–327.
13. Echelard Y, Vassileva G, McMahon AP (1994) Cis-acting regulatory sequences governing Wnt-1 expression in the developing mouse CNS. *Development* 120:2213–2224.
14. Le Douarin NM, Fontaine-Pérus J, Couly G (1986) Cephalic ectodermal placodes and neurogenesis. *Trends Neurosci* 9:175–180.
15. Begbie J, Brunet J-F, Rubenstein JL, Graham A (1999) Induction of the epibranchial placodes. *Development* 126:895–902.

16. Yntema CL (1944) Experiments on the origin of the sensory ganglia of the facial nerve in the chick. *J Comp Neurol* 81:147–167.
17. Begbie J, Graham A (2001) Integration between the epibranchial placodes and the hindbrain. *Science* 294:595–598.
18. Kucenas S, et al. (2008) CNS-derived glia ensheath peripheral nerves and mediate motor root development. *Nat Neurosci* 11:143–151.
19. Zechner D, et al. (2003) β-Catenin signals regulate cell growth and the balance between progenitor cell expansion and differentiation in the nervous system. *Dev Biol* 258:406–418.
20. Pattyn A, Hirsch M-R, Goridis C, Brunet J-F (2000) Control of hindbrain motor neuron differentiation by the homeobox gene *Phox2b*.. *Development* 127:1349–1358.
21. Bruesch SR (1944) The distribution of myelinated afferent fibers in the branches of the cat's facial nerve. *J Comp Neurol* 81:169–191.
22. Fode C, et al. (1998) The bHLH protein NEUROGENIN 2 is a determination factor for epibranchial placode-derived sensory neurons. *Neuron* 20:483–494.
23. Pattyn A, Morin X, Cremer H, Goridis C, Brunet J-F (1997) Expression and interactions of the two closely related homeobox genes *Phox2a* and *Phox2b* during neurogenesis. *Development* 124:4065–4075.
24. Dauger S, et al. (2003) Phox2b controls the development of peripheral chemoreceptors and afferent visceral pathways. *Development* 130:6635–6642.
25. Berger J, et al. (2004) E1-Ngn2/Cre is a new line for regional activation of Cre recombinase in the developing CNS. *Genesis* 40:195–199.
26. Srinivas S, et al. (2001) Cre reporter strains produced by targeted insertion of EYFP and ECFP into the ROSA26 locus. *BMC Dev Biol* 1:4.
27. Graham A, Blentic A, Duque S, Begbie J (2007) Delamination of cells from neurogenic placodes does not involve an epithelial-to-mesenchymal transition. *Development* 134: 4141–4145.
28. Ericson J, Thor S, Edlund T, Jessell TM, Yamada T (1992) Early stages of motor neuron differentiation revealed by expression of homeobox gene *Islet-1*. *Science* 256: 1555–1560.
29. Avivi C, Goldstein RS (1999) Differential expression of Islet-1 in neural crest-derived ganglia: Islet-1 + dorsal root ganglion cells are post-mitotic and Islet-1 + sympathetic ganglion cells are still cycling. *Brain Res Dev Brain Res* 115:89–92.
30. Parlato R, Otto C, Begus Y, Stotz S, Schütz G (2007) Specific ablation of the transcription factor CREB in sympathetic neurons surprisingly protects against developmentally regulated apoptosis. *Development* 134:1663–1670.
31. Pattyn A, et al. (2004) Ascl1/Mash1 is required for the development of central serotonergic neurons. *Nat Neurosci* 7:589–595.
32. Sommer L, Ma Q, Anderson DJ (1996) Neurogenins, a novel family of atonal-related bHLH transcription factors, are putative mammalian neuronal determination genes that reveal progenitor cell heterogeneity in the developing CNS and PNS. *Mol Cell Neurosci* 8:221–241.
33. Fitzgerald MJ, Alexander RW (1969) The intramuscular ganglia of the cat's tongue. *J Anat* 105:27–46.
34. Verberne ME, Gittenberger-de Groot AC, Poelmann RE (1998) Lineage and development of the parasympathetic nervous system of the embryonic chick heart. *Anat Embryol (Berl)* 198:171–184.
35. Tollet J, Everett AW, Sparrow MP (2001) Spatial and temporal distribution of nerves, ganglia, and smooth muscle during the early pseudoglandular stage of fetal mouse lung development. *Dev Dyn* 221:48–60.
36. Gibbins I (1994) *Comparative Physiology and Evolution of the Autonomic Nervous system*, eds Nisson S, Holmgren S (Harvard Academic Publishers, Boston), pp 1–67.
37. Dufour HD, et al. (2006) Precraniate origin of cranial motoneurons. *Proc Natl Acad Sci USA* 103:8727–8732.
38. Rodríguez CI, et al. (2000) High-efficiency deleter mice show that FLPe is an alternative to Cre-loxP. *Nat Genet* 25:139–140.
39. Hippenmeyer S, et al. (2005) A developmental switch in the response of DRG neurons to ETS transcription factor signaling. *PLoS Biol* 3:e159.
40. Tiveron MC, Hirsch MR, Brunet JF (1996) The expression pattern of the transcription factor Phox2 delineates synaptic pathways of the autonomic nervous system. *J Neurosci* 16:7649–7660.
41. Knittel T, Kessel M, Kim MH, Gruss P (1995) A conserved enhancer of the human and murine *Hoxa-7* gene specifies the anterior boundary of expression during embryonal development. *Development* 121:1077–1088.
42. Sillitoe RV, Hawkes R (2002) Whole-mount immunohistochemistry: a high-throughput screen for patterning defects in the mouse cerebellum. *J Histochem Cytochem* 50: 235–244.